Dimethylacetamide-Based Eutectic Electrolyte for High-Performance Aqueous Lithium-Ion Batteries

Jiajie Zhang,[a] Changkun Zhang*[a]

[a] Division of Energy Storage, Dalian National Laboratory for Clean Energy, *i*ChEM (Collaborative Innovation Center of Chemistry for Energy Materials), Dalian Institute of Chemical Physics, Chinese Academy of Sciences, Dalian 116023, China

*Corresponding author. E-mail:zhangchk17@dicp.ac.cn

Materials and methods

Materal

Poly(vinylidene fluoride) (PVDF) with a molecular weight (Mw) of 455000, was obtained from Sigma-Aldrich Co., Ltd. N-methyl-2-pyrrolidone (NMP, 99.9% purity) were sourced from Beijing InnoChem Science & Technology Co., Ltd. The $LiMn_2O_4$ (LMO) and $Li_4Ti_5O_{12}$ (LTO) powder was purchased from Hefei Kejing Materials Technology Co., Ltd. Lithium bis(fluorosulfonyl)imide (LiFSI) was purchased from Shenzhen Capchem Co., Ltd. The separator is produced by Celgard LLC Co., Ltd. (model: Celgard3501).

Preparation of cathode and anode

To prepare the LMO cathode, a homogeneous slurry was prepared by blending 80 wt% LMO powder, 10 wt% Super P carbon, and 10 wt% PVDF binder in NMP through continuous stirring. The mixture was then evenly distributed onto an aluminum foil substrate using the doctor-blade method and then vacuum dried at 80 C for 12 h, yielding LMO cathodes with areal mass loading of approximately 2.2 and 10 mg cm^{-2}. To prepare the LTO cathode, a homogeneous slurry was prepared by blending 80 wt% LTO powder, 10 wt% Super P carbon, and 10 wt% PVDF binder in NMP through continuous stirring. The mixture was then evenly distributed onto a copper foil substrate using the doctor-blade method and then vacuum dried at 80 C for 12 h, yielding LTO cathodes with areal mass loading of approximately 1.1 and 5 mg cm^{-2}. Use electrodes with a lower loading (1.1 mg cm^{-2} LTO and 2.2 mg cm^{-2} LMO) at -20^{o}C.

Battery assembly

The battery assembly process took place within an argon-filled glovebox to ensure the oxygen and water contents remained below 0.1 ppm. LMO/LTO full cells with different electrolytes and celgard 3501 membrane were assembled in CR2032-type coin cells.

Material characterizations

To analyze the interactions among different components in the electrolyte, Fourier transform-infrared spectroscopy (FTIR) was performed on Thermo Scientific Nicolet

iS10 spectrometer. The electrochemical impedance spectroscopy (EIS) was measured after the discharge is completed in the range of 100 kHz-0.01 Hz using an electrochemical workstation VSP-300 (Biologic, France). To investigate the interfacial chemistry of the LMO, X-ray photoelectron spectroscopy (XPS, Thermo Fisher Scientific) was performed using monochromatic Al Kα radiation (1486.6 eV) as an X-ray source. Time-of-flight secondary ion mass spectrometry (TOF-SIMS) was performed to obtain the depth profile of the LTO electrode on TOF-SIMS M6 (IONTOF GmbH). To analyze the gas generation during the charging and discharging process of batteries, differential electrochemical mass spectrometry (DEMS, Hider) was performed with in-situ electrochemical cell.

Theoretical calculation

Materials Studio tool is applied for the Molecular dynamics (MD) calculations. An amorphous cubic cell with 10 LiFSI, 5 H_2O and 40 DMAC molecules is constructed for LiFSI: H_2O: DMAC recipe simulation. Geometry optimization is applied in Forcite package with COMPASS III forcefield assigned. NVT canonical ensemble is chosen for dynamic simulation at 298K with Nose thermostat and 1fs time step for total 1000 ps duration.

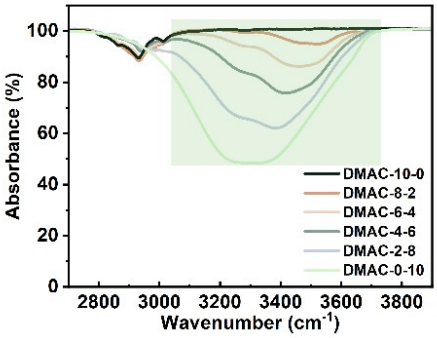

Figure S1. The H-O stretching vibration peaks of FTIR for DMAC-H_2O mixed solutions of different molar ratio.

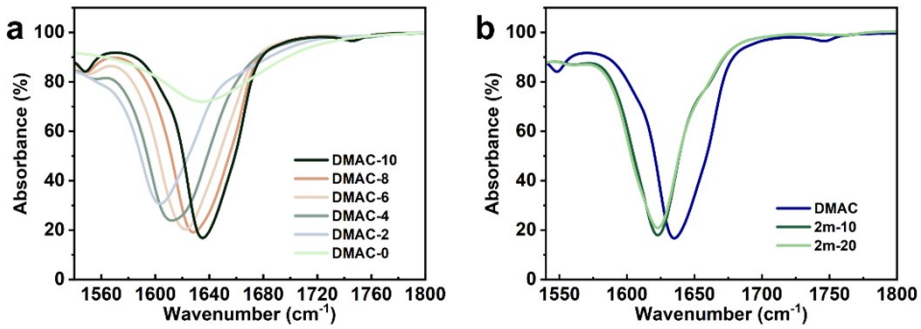

Figure S2. The C=O stretching vibration peaks of FTIR for (a) DMAC-H_2O solutions with different molar ratios and (b) DMAC, 2m-10 and 2m-20.

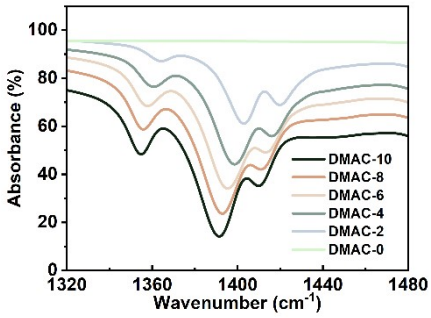

Figure S3. The C-H vibration peaks of FTIR for DMAC-H_2O mixed solutions of different molar ratios.

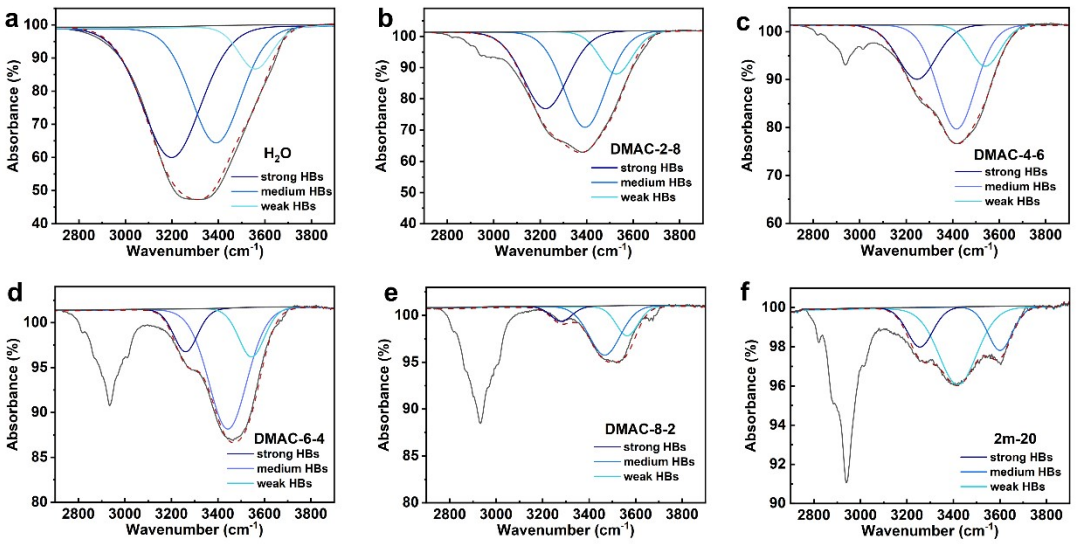

Figure S4. The H-O stretching vibration peaks of (a) H_2O, (b) DMAC-2-8, (c) DMAC-4-6, (d) DMAC-6-4, (e) DMAC-8-2 and (f) 2.5m-20 are deconvoluted into strong HBs, medium HBs and weak HBs.

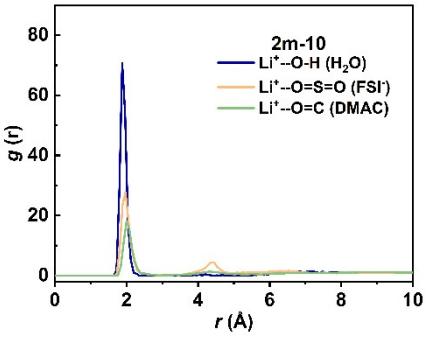

Figure S5. RDF of 2m-10.

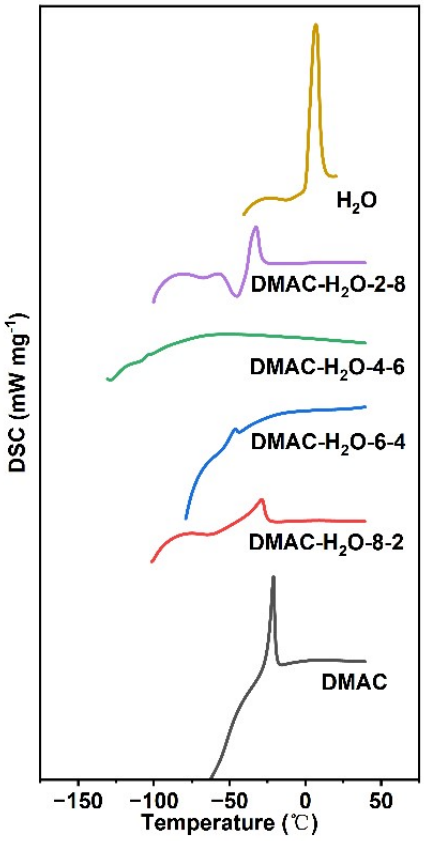

Figure S6. DSC curves of DMAC-H_2O solutions with different molar ratios.

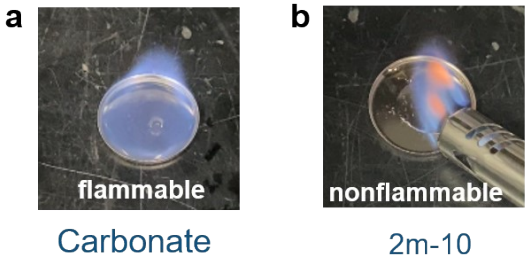

Figure S7. The flame retardancy of (a) commercial carbonate-based electrolytes and (b) 2m-10 when exposed to flame contact.

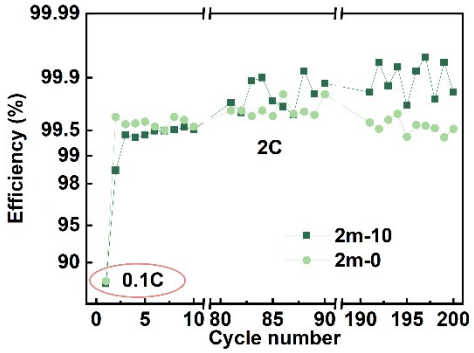

Figure S8. The CE of LMO||2m-10||LTO and LMO||2m-0||LTO at 1-10, 80-90 and 190-200 cycles.

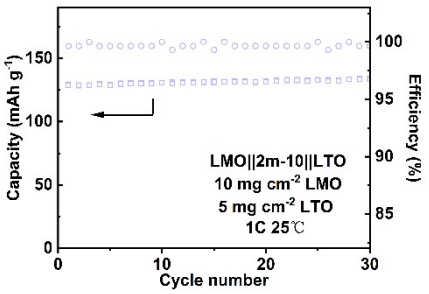

Figure S9. The cycle performance of high-capacity full cells at 1C.

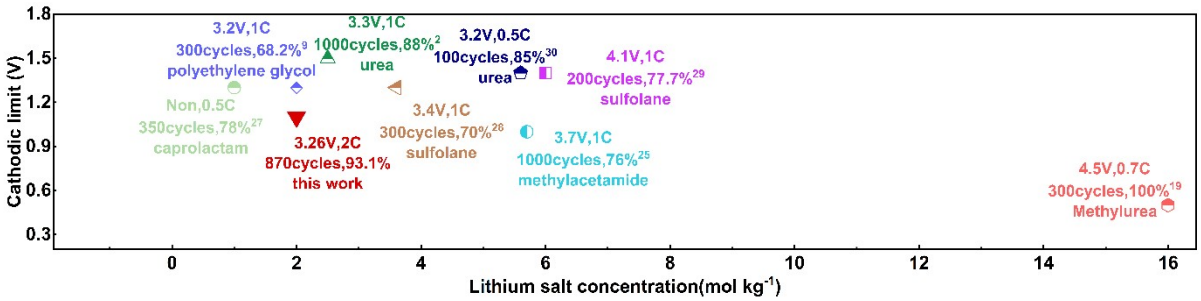

Figure S10. A comparative of battery performance with different eutectic molecule, cathodic limit, lithium salt concentration and electrochemical window across different article.

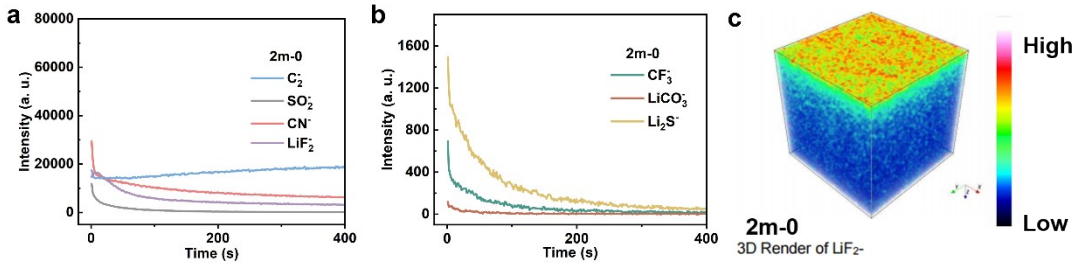

Figure S11. TOF-SIMS depth profiles of C_2^-, SO_2^-, CN^-, LiF_2^-, CF_3^-, $LiCO_3^-$ and Li_2S^-secondary ions on the cycled LTO in 2m-0 and (e) 3D image of the LTO in 2m-0.

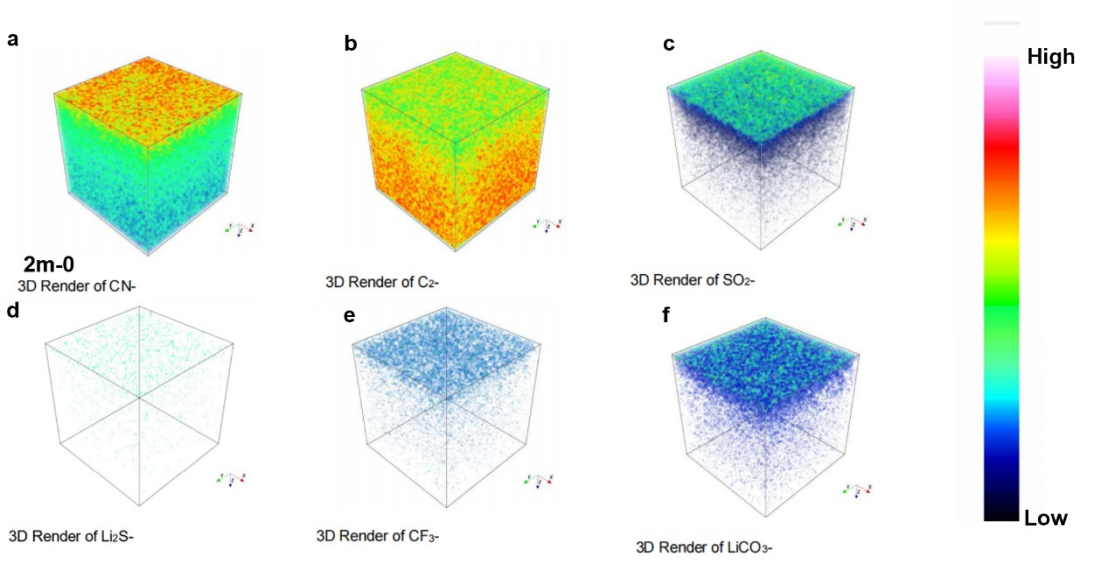

Figure S12. TOF-SIMS 3D image of (a) CN^-, (b) C_2^-, (c) SO_2^-, (d) Li_2S^-, (e) CF_3^- and (f) $LiCO_3^-$ of LTO cycled in 2m-0 electrolyte.

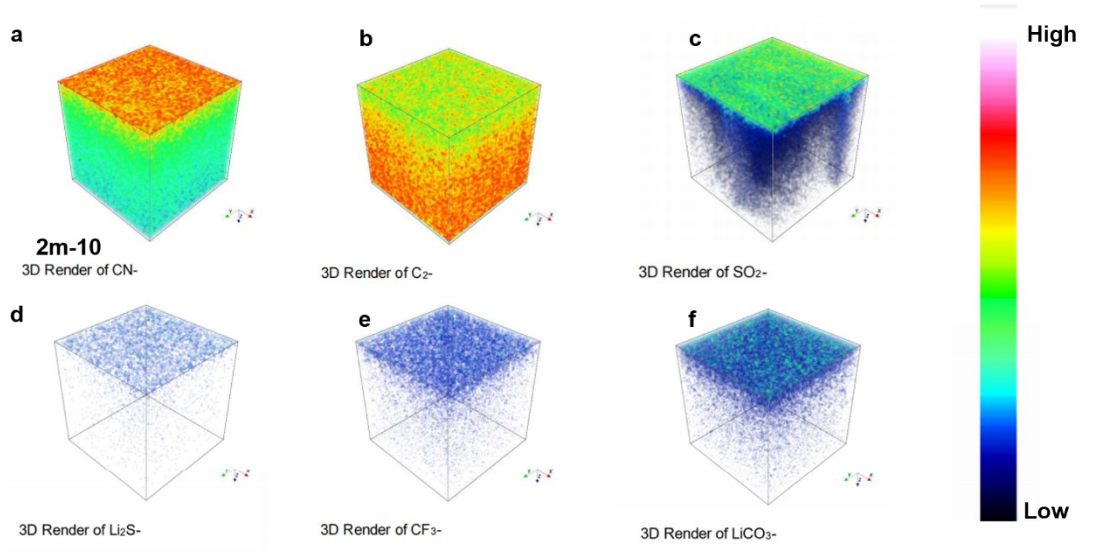

Figure S13. TOF-SIMS 3D image of (a) CN^-, (b) C_2^-, (c) SO_2^-, (d) Li_2S^-, (e) CF_3^- and (f) $LiCO_3^-$ of LTO cycled in 2m-10 electrolyte.

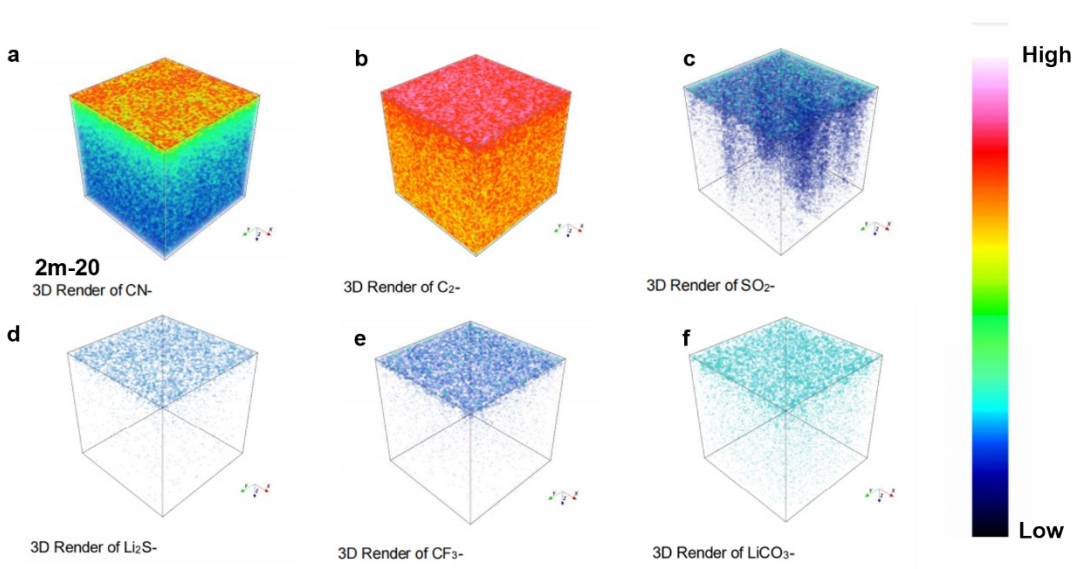

Figure S14. TOF-SIMS 3D image of (a) CN^-, (b) C_2^-, (c) SO_2^-, (d) Li_2S^-, (e) CF_3^- and (f) $LiCO_3^-$ of LTO cycled in 2m-20 electrolyte.

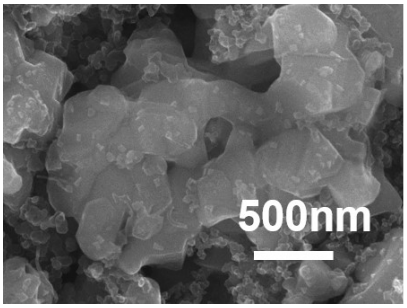

Figure S15. SEM images of LTO cycled in 2m-10.

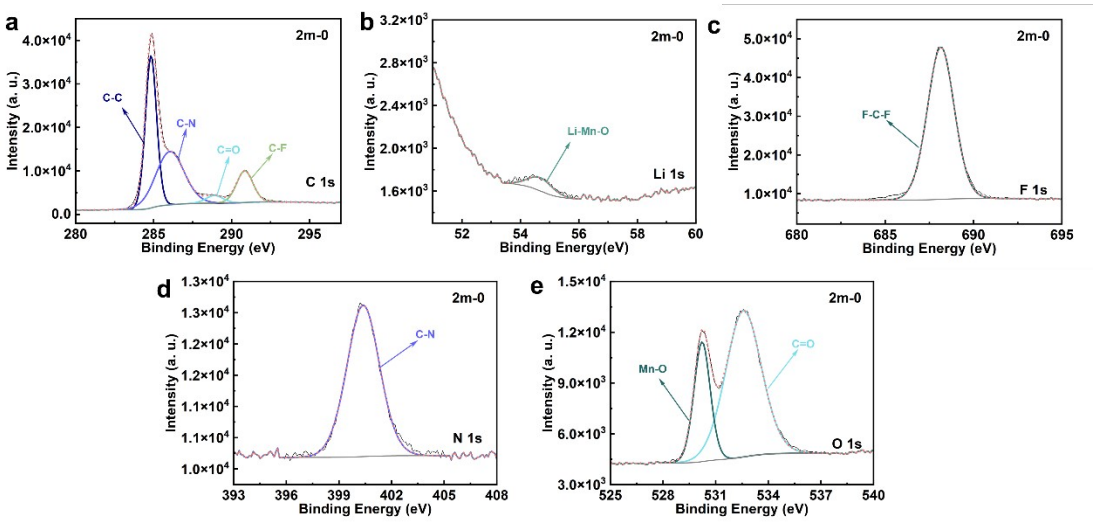

Figure S16. XPS results for (a) C 1s, (b) Li 1s, (c) F 1s, (d) N1s and (e) O1s of the LMO in 2m-0 electrolyte.

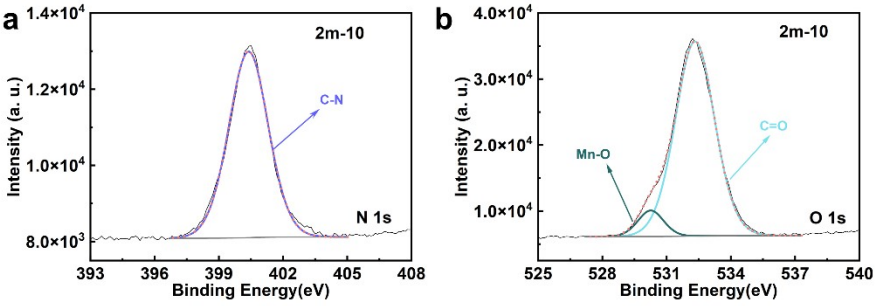

Figure S17. XPS results for (a) N1s and (b) O1s of the LMO in 2m-10 electrolyte.

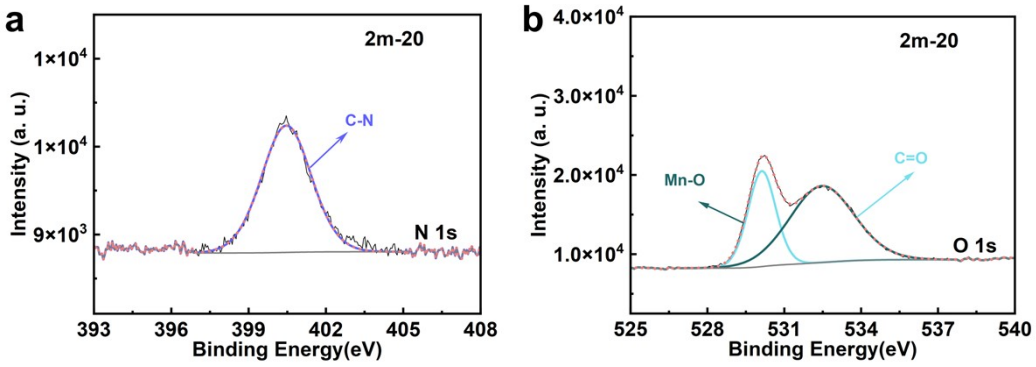

Figure S18. XPS results for (a) N1s and (b) O1s of the LMO in 2m-20 electrolyte.